American Mineralogist, Volume 97, pages 262–267, 2012

Thermal elastic behavior of $CaSiO_3$-walstromite: A powder X-ray diffraction study up to 900 °C

Xi Liu,[1,*] Sicheng Wang,[1] Qiang He,[1] Jinlan Chen,[1] Hejing Wang,[1] Sichen Li,[1] Fang Peng,[2] Lifei Zhang,[1] and Yingwei Fei[1,3]

[1]The Key Laboratory of Orogenic Belts and Crustal Evolution, Ministry of Education of China; School of Earth and Space Sciences, Peking University, Beijing 100871, China
[2]Institute of Atomic and Molecular Physics, Sichuan University, Chengdu 610065, China
[3]Geophysical Laboratory, Carnegie Institution of Washington, 5251 Broad Branch Road, NW, Washington, D.C. 20015, U.S.A.

Abstract

Walstromite-structured $CaSiO_3$ (Wal) was synthesized at 6 GPa and 1200 °C for 6 h using a cubic press, and its thermal elastic behavior was investigated at T up to 900 °C using a powder X-ray diffraction technique at ambient pressure. Within the investigated T range, all unit-cell parameters, j, of Wal varied almost linearly with T, so that we fitted the data with the equation $\alpha_j = j^{-1}(\partial j/\partial T)$ and obtained $\alpha_a = 0.92(2) \times 10^{-5}$/°C, $\alpha_b = 1.65(1) \times 10^{-5}$/°C, $\alpha_c = 0.83(1) \times 10^{-5}$/°C, and $\alpha_V = 3.24(3) \times 10^{-5}$/°C for Wal. The magnitudes of the principal Lagrangian strain coefficients (ε_1, ε_2, and ε_3) and the orientation of the thermal strain ellipsoids, between ambient T and measured T, were calculated. The orientation of the strain ellipsoid appears constant with T variation, whereas the strain magnitudes vary significantly with T: ε_1 increases, but ε_2 and ε_3 decrease. For T > 900 °C, primitive data were collected for "parawollastonite" (Wo-2M), which led to a much smaller volumetric thermal expansion coefficient than that of Wal.

Keywords: $CaSiO_3$-walstromite, high-P synthesizing, high-T X-ray diffraction, "parawollastonite", thermal elasticity

Introduction

It has been well accepted by the scientific community that the mantle of the Earth is mainly peridotitic (pyrolite; Ringwood 1975), with some minor portions being eclogitic due to the recycling of the oceanic crust back to the deep interior of the Earth via the subduction process (Ringwood 1994; Hirose et al. 1999). Recently, many Ca-silicate phases such as walstromite-structured $CaSiO_3$ (Wal), titanite-structured $CaSi_2O_5$ (Ttn), and larnite (β-Ca_2SiO_4; Lrn) were discovered as inclusions in diamonds that probably originated from the lower mantle (Joswig et al. 1999; Jambor et al. 2000; Stachel et al. 2000; Nasdala et al. 2003; Brenker et al. 2005), indicating a potential Ca-rich lithology in the Earth's deep mantle. Trace element analyses of these Ca-rich inclusions suggested extreme degrees of LREE (200–2000 times chondritic) and Sr enrichment (70–1000 times chondritic) together with negative and positive Eu anomalies (Stachel et al. 2000), suggesting that this Ca-rich lithology might be an important reservoir with distinctive geochemical features. For a better understanding of the physical-chemical interaction among these different lithologies in the deep interior of the Earth, it is apparently very important to study these Ca-rich phases.

To understand the geodynamic process that these natural Ca-rich inclusions in diamonds once experienced, the phase relationships in the composition $CaSiO_3$ at high P-T conditions are critical; these are well understood: Wal, Ttn, and Lrn are related by the reaction 3Wal = Ttn + Lrn, which takes place at about 8 GPa (Kanzaki et al. 1991; Wang and Weidner 1994; Gasparik et al. 1994; Kubo et al. 1997; Akaogi et al. 2004; Sueda et al. 2006). At a lower pressure of about 3 GPa (Essene 1974; Huang and Wyllie 1975; Chatterjee et al. 1984; Akaogi et al. 2004), Wal transforms to wollastonite-I (Wo; $CaSiO_3$; Barkley et al. 2011). At a higher pressure of about 12 GPa, Ttn and Lrn combine to form $CaSiO_3$-perovskite, the dominant Ca-bearing phase in the lower mantle of the Earth (Mao et al. 1977; Irifune et al. 1989; Tamai and Yagi 1989). To appreciate the incorporation of the trace elements, such as LREE and Sr, in these Ca-rich phases, on the other hand, detailed crystallographic and thermal elastic data are required (Blundy and Wood 1994; Law et al. 2000). As outlined by Swamy and Dubrovinsky (1997a) and Akaogi et al. (2004), however, many thermal elastic properties of Wal, Ttn, and Lrn have not been experimentally determined so far.

Wal ($CaSiO_3$; $P\bar{1}$) was first synthesized by Ringwood and Major (1967), with its first structure determination by Trojer [1969; a = 6.695(5), b = 9.257(7), c = 6.666(6) Å, α = 86°38′, β = 76°08′, γ = 70°23′]. Joswig et al. (2003) detailed the crystal structure of Wal entrapped as inclusion in diamond by single-crystal X-ray diffraction, and also predicted its compression behavior up to about 35 GPa using density functional theory. Here we have investigated the thermal elasticity of Wal by powder X-ray diffraction at T up to ~900 °C.

* E-mail: xi.liu@pku.edu.cn

0003-004X/12/0203–262$05.00/DOI: http://dx.doi.org/10.2138/am.2012.3918

EXPERIMENTAL METHODS

The polycrystalline Wal sample used in our high-*T* powder X-ray diffraction experiments was synthesized with a CS-IV 6×14 MN cubic press recently installed at the High-Pressure Laboratory of Peking University. The pressurization system of this press consists of six WC anvils, with their tips truncated as 23.5 × 23.5 mm^2, which are simultaneously pushed by six hydraulic rams so that high pressure is generated in the experimental assembly. The experimental assembly, BJC-1, used in this study, is schematically illustrated in Figure 1, and its pressure calibration at room temperature is shown in Figure 2. The experimental *T* was measured and controlled with a $Pt_{94}Rh_6$-$Pt_{70}Rh_{30}$ thermocouple (type B), ignoring any potential pressure effect on its e.m.f.; since the thermocouple was located ~4 mm from the center of the assembly (Fig. 1), the center of the sample may be ~100 °C higher than the thermocouple reading. The starting material for the synthesizing experiments was prepared as follows: we first mixed under acetone the powders of SiO_2 and $CaCO_3$ in a molar ratio of 1:1; second, pressed this mixture into a pellet and degassed it at 1 atm and 1000 °C for about 48 h; third, crushed the pellet into a fine powder under acetone that was used later. The starting material was sealed in an *h*BN capsule. The synthesizing *P-T* conditions were 6 GPa and 1200 °C for 6 h (Gasparik et al. 1994; Swamy and Dubrovinsky 1997a; Akaogi et al. 2004; Sueda et al. 2006). In total, we conducted three high-*P* synthesizing experiments to generate enough material for later high-*T* X-ray diffraction experiments. The synthetic products from the high-*P* experiments were examined by a scanning electron microscope (SEM; Quanta 200 FEG) and electron microprobe analysis (EMPA; JEOL JXA-8100), and finely ground under acetone in an agate mortar.

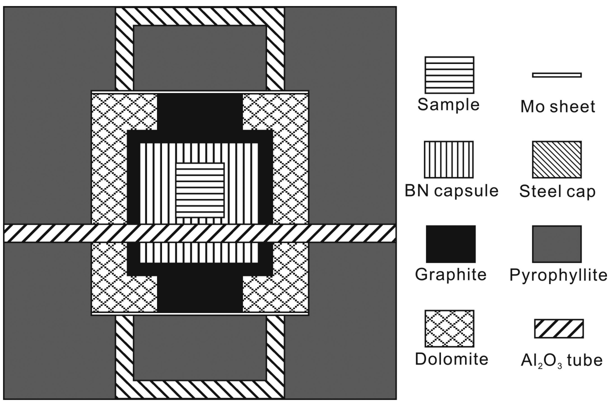

FIGURE 1. Experimental assembly (BJC-1; not to scale) used in the high-*P* synthesizing experiments with the cubic press CS-IV 6×14 MN installed at the High-Pressure Laboratory, Peking University.

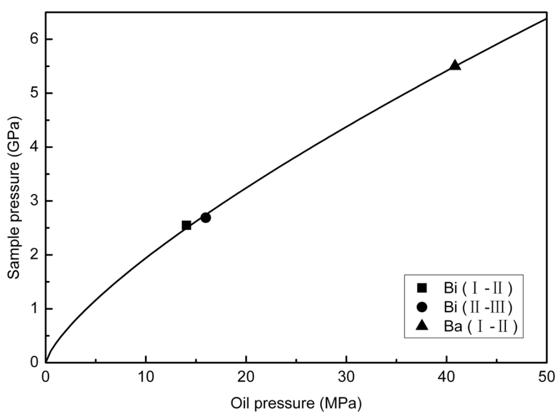

FIGURE 2. Experimental pressure vs. oil pressure at ambient temperature for the experimental assembly BJC-1. Metals Bi and Ba were used in the pressure calibration.

In the high-*T* X-ray diffraction experiments performed at ambient *P*, we used an X'Pert Pro MPD system, which had an attached Anton Paar HTK-1200N oven running with a Eurotherm temperature controller (Eurotherm 2604; type S thermocouple checked against the melting point of NaCl). With this heating system, we can reach 1200 °C with an accuracy of ±2 °C (Liu et al. 2010, 2011; Hu et al. 2011). Other details of the X'Pert Pro MPD diffractometer system include a Cu target, operation voltage of 40 kV and current of 40 mA. High-*T* experiments were conducted up to 1000 °C with heating rates of 10 °C/min and thermal equilibration times of 5 min. Since the phase transition from Wal to wollastonite-I is generally quick (Essene 1974), long data-collection times at high *T* should be avoided. Therefore, we only collected the X-ray data between 9 and 70 °2θ, with a scanning step length of 0.017 °2θ and a scanning time of 10 s for each scanning step. In addition, we found later that the X-ray peaks between 50 and 70 °2θ were not only weak, but also severely overlapping, due to the low symmetry and the large unit-cell parameters of Wal, so that they were not very usable for the determination of the unit-cell parameters. The alignment of the X-ray diffractometer system was performed at ambient *T* with a standard crystalline Si powder. Due to the thermal expansion of the furnace, the sample holder components, and the powder sample itself, the sample position slightly changed at high *T*. Following the data-processing procedure demonstrated in Hu et al. (2011), we used the MDI program Jade 5.0 (Material Data, Inc.) to correct the influence of the small sample displacement by a full powder X-ray pattern refinement (between 9 and 50 °2θ), which led to unit-cell parameters with high accuracy.

RESULTS AND DISCUSSION

High-*T*, ambient-*P* X-ray diffraction experiments were conducted up to 1000 °C (Fig. 3). We found that all X-ray diffraction peaks observed for *T* < 800 °C belonged to Wal (Trojer 1969; Joswig et al. 2003; Barkley et al. 2011), and the new peaks appearing from 800 °C on could be attributed to the low-pressure phase Wo-I, or, more precisely, the 2*M* polytype of Wollastonite-I (Wo-2*M*, historically known as "parawollastonite"; Trojer 1968; Ohashi 1984; Hesse 1984). For *T* < 1125 °C and 1 atm, there are many polytypes of Wollastonite-I such as Wo-1*T*, Wo-3*T*, Wo-4*T*, Wo-5*T*, Wo-7*T*, and Wo-2*M* (Wenk 1969; Henmi et al. 1978, 1983; Mazzucato and Gualtieri 2000), among which Wo-2*M* is probably the corresponding high-*T* form (Henmi et al. 1983; Mazzucato and Gualtieri 2000). These polytypes of $CaSiO_3$ at *T* < 1125 °C have been given different names such as *β*-wollastonite, wollastonite-I, and $CaSiO_3$ (I) (Barkley et al.

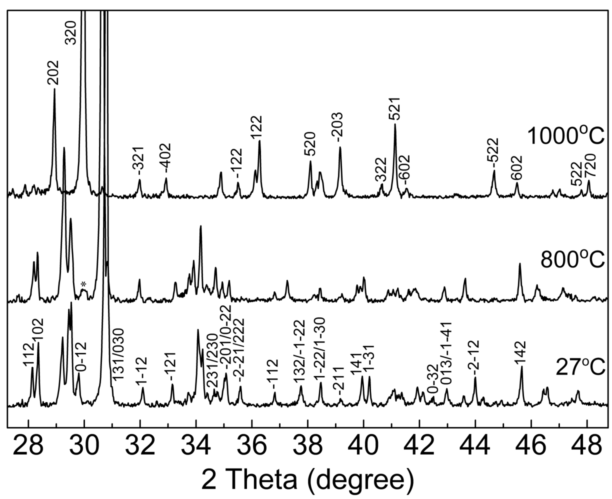

FIGURE 3. XRD patterns collected at 27, 800, and 1000 °C. At 800 °C, one X-ray diffraction peak that belongs to Wo-2*M* started to appear, as indicated by the asterisk.

2011). Presumably due to the relatively low *T* and short heating duration in our X-ray diffraction experiments, no polytype other than Wo-2*M* grew from Wal. On the other hand, "pseudowollastonite" of different polytypes (PsWo; Yamanaka and Mori 1981; Ingrin 1993; Yang and Prewitt 1999a, 1999b), which have been collectively termed α-wollastonite (Yamanaka and Mori 1981), is only stable at $T > 1125$ °C (Kushiro 1964; Essene 1974; Mikirticheva et al. 2001), so that we could not observe any diffraction peaks for this phase at any *T*. Nevertheless, the phase transition from Wal to Wo-2*M* was not completed until 950 °C, and most X-ray diffraction peaks of Wal were still observed up to 900 °C and could be used to extract its unit-cell parameters. The derived unit-cell parameters of Wal from the X-ray diffraction patterns as a function of *T* are listed in Table 1. As to Wo-2*M*, we obtained its unit-cell parameters as following: at 950 °C, $a = 15.55(2)$, $b = 7.365(8)$, $c = 7.082(8)$ Å, $\beta = 95.18(6)°$, and $V = 808(2)$ Å^3; at 1000 °C, $a = 15.62(2)$, $b = 7.373(6)$, $c = 7.096(6)$ Å, $\beta = 95.28(7)°$, and $V = 813(1)$ Å^3.

The variation of the unit-cell parameters of Wal with *T* (Figs. 4 and 5) is generally linear for the investigated *T* range. With the exception of the γ angle, all other parameters increase as *T* increases. The anisotropic thermal elasticity for Wal is demonstrated in the data over the range 27 to 900 °C: the *a*-axis increases by 0.82%, the *b*-axis by 1.42%, and the *c*-axis by 0.76%. The room-*P* unit-cell parameters of Wal as a function of *T* have been fitted with the equation $j = j_0 e^{\alpha j(T-T_0)}$ to derive the thermal expansion coefficients $\alpha_j = j^{-1}(\partial j/\partial T)$, where *j* stands for *a*, *b*, *c*, or *V*. The derived thermal expansion coefficients are listed in Table 2 and compared with those of Wo and PsWo (Swamy et al. 1997b; Richet et al. 1998). It should be noted that the nature of the polytype(s) of the Wo sample investigated by Swamy et al. (1997b) was not completely clear, although the Wo-1*T* polytype might be the predominant form. Similarly, the study of PsWo done by Richet et al. (1998) had the same problem in their sample (Ingrin 1993). To facilitate the following comparison, we hereafter ignore the complexity in the polytypes of their investigated samples. Due to the small difference in the free energies of the different polytypes of $CaSiO_3$ at 1 atm, the rates of the polymorphic phase transitions are rather slow, and the exact phase relationship has not been experimentally determined yet.

TABLE 1. Unit-cell parameters of Wal vs. *T*

T (°C)	*a* (Å)	*b* (Å)	*c* (Å)	α (°)	*β* (°)	*γ* (°)	*V* (Å^3)
27	6.691(1)	9.2958(1)	6.6529(6)	83.76(1)	76.21(1)	69.66(1)	376.67(8)
50	6.692(2)	9.2998(1)	6.6556(8)	83.74(2)	76.23(1)	69.68(1)	377.1(1)
100	6.695(1)	9.3049(1)	6.6557(4)	83.75(1)	76.24(1)	69.62(0)	377.34(7)
150	6.696(1)	9.3123(1)	6.6597(4)	83.81(1)	76.27(1)	69.60(1)	377.94(5)
200	6.704(2)	9.3213(1)	6.6618(6)	83.84(1)	76.29(1)	69.56(1)	378.83(9)
250	6.708(1)	9.3313(1)	6.6658(1)	83.87(1)	76.30(1)	69.52(1)	379.6(1)
300	6.712(3)	9.3401(1)	6.670(1)	83.89(2)	76.31(2)	69.47(2)	380.3(2)
350	6.713(2)	9.3440(1)	6.670(1)	83.96(2)	76.36(2)	69.47(2)	380.7(1)
400	6.716(1)	9.3507(1)	6.673(1)	83.97(1)	76.36(1)	69.41(1)	381.2(1)
450	6.718(2)	9.3594(1)	6.6737(7)	84.06(2)	76.42(1)	69.39(1)	381.7(1)
500	6.718(1)	9.3670(1)	6.6779(1)	84.12(1)	76.45(1)	69.37(1)	382.26(8)
550	6.724(2)	9.3773 (1)	6.6808(1)	84.18(2)	76.47(1)	69.32(1)	383.0(1)
600	6.724(2)	9.3849 (1)	6.6838(9)	84.23(1)	76.51(1)	69.26(1)	383.5(1)
650	6.727(2)	9.3898(1)	6.6864(9)	84.28(2)	76.55(1)	69.25(1)	384.1(1)
700	6.730(1)	9.3988(1)	6.6911(6)	84.35(1)	76.58(1)	69.23(1)	384.88(7)
750	6.732(2)	9.4069(1)	6.6945(8)	84.39(1)	76.61(1)	69.20(1)	385.5(1)
800	6.737(1)	9.4080(10)	6.6954(7)	84.43(1)	76.61(1)	69.22(1)	385.9(1)
850	6.739(3)	9.4214(1)	6.700(1)	84.47(2)	76.66(1)	69.12(1)	386.7(2)
900	6.746(1)	9.4278(1)	6.704(1)	84.56(1)	76.74(2)	69.10(2)	387.6(1)

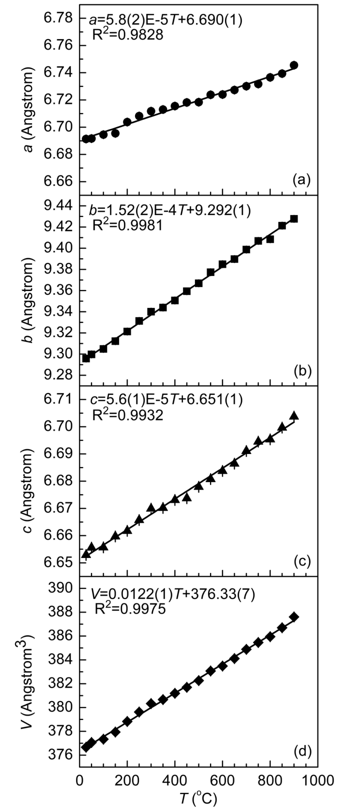

FIGURE 4. Variation of the unit-cell parameters of Wal with *T*: (**a**) the *a*-axis; (**b**) the *b*-axis; (**c**) the *c*-axis; (**d**) the volume. Note that lengths of the error bars are generally equal to or smaller than the symbols.

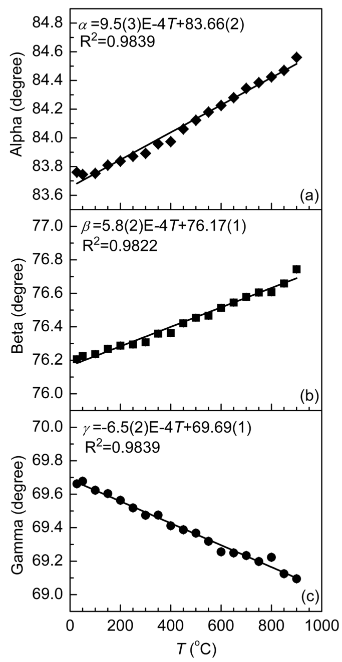

FIGURE 5. Variation of the unit-cell parameters of Wal with *T*: (**a**) the angle α; (**b**) the angle β; (**c**) the angle γ. Note that lengths of the error bars are generally equal to or smaller than the symbols.

TABLE 2. Thermal expansion coefficients of Wal, Wo, and PsWo at ambient *P*

Phase	α_a(10^{-5}/°C)	α_b(10^{-5}/°C)	α_c(10^{-5}/°C)	α_V(10^{-5}/°C)	Data source
Wal	0.92(2)	1.65(1)	0.83(2)	3.24(3)	This study
Wo	1.108(0)	1.065(0)	1.070(0)	3.123(0)	Swamy et al. (1997b)*
PsWo	1.02(7)	1.2(1)	0.86(8)	3.1(2)	Richet et al. (1998)†

* Unit-cell parameters up to 1000 °C calculated using their equations, processed by our method.
† Experimental measurements up to 992 °C processed by our equation.

For the interval from ambient *T* to about 1000 °C, α_V of these three polymorphic phases are almost identical and have little *T*-dependence, with that of Wal being only about 3% larger than those of Wo and PsWo (Table 2). Swamy et al. (1997a) thermodynamically estimated the thermal expansion coefficients of Wal and PsWo, and compared them to those of Wo experimentally constrained by Swamy et al. (1997b). Their investigation suggested that α_V of PsWo at ambient *T* is about 70% larger than that of Wal or Wo (Table 5c of Swamy et al. 1997a), which disagrees with our observation (Table 2). It follows that, with the new thermal expansion data of PsWo from Richet et al. (1998) and of Wal from this study, the thermodynamic data set of Swamy et al. (1997a) for the phases in the $CaSiO_3$ system should be further refined.

By putting together our *V-T* data for Wo-2*M* at high *T* with those at ambient *T* (25 °C; Ohashi 1984; Hesse 1984), we tentatively obtain for Wo-2*M* $\alpha_a = 1.13(4) \times 10^{-5}$/°C, $\alpha_b = 0.67(7) \times 10^{-5}$/°C, $\alpha_c = 0.34(3) \times 10^{-5}$/°C, and $\alpha_V = 2.2(6) \times 10^{-5}$/°C. Therefore, it is clear that α_V of Wo-2*M* << α_V of Wal, Wo, and PsWo (Table 2). Due to the limited numbers of the unit-cell parameters, however, the thermal expansion coefficients of Wo-2*M* estimated here should be viewed as being semi-quantitative only.

Additionally, the axial thermal expansion of Wal is strongly anisotropic (α_a:α_b:α_c = 1.1:2.0:1). The much larger thermal expansivity along the *b*-axis is highly possibly related to the continuous CaO layers, which run parallel to the *b*-axis (Fig. 6). In contrast, the ratios of α_a:α_b:α_c for Wo and PsWo are 1.04:1:1 and 1.19:1.40:1, respectively, indicating less prominent elastic anisotropy for these two phases. Joswig et al. (2003) used the density functional theory to investigate the compression behavior of Wal, and reached the conclusion that the elastic anisotropy of Wal was rather small. To resolve this potential discrepancy in the elasticity of Wal, direct compression experiments under high pressure appear desirable.

Wal is triclinic with space group $P\bar{1}$, so the orientation of the principal strain axes is arbitrary in the crystal's frame. Using the STRAIN program (Ohashi 1982), we calculated the magnitudes of the Lagrangian principal strain coefficients (ε_1, ε_2, and ε_3) between the ambient *T* (27 °C) and each measured *T*, as well as the orientation of the thermal strain ellipsoids (Table 3). The orientation of the strain ellipsoid appears to be approximately constant with *T*. In contrast, the evolution of the strain magnitudes with increasing *T*, as displayed in Figure 7, is not constant at all: ε_1 increases, whereas ε_2 and ε_3 decrease. Since ε_1 is larger than ε_2 and ε_3 at ambient *T*, high *T* elongates the principal strain ellipsoid of Wal. This increasing thermal elastic anisotropy is clearly indicated by the strain coefficients summarized in Table 3: for instance, the anisotropy between 27 and 200 °C is ε_1:ε_2:ε_3 = 3.7:1.2:1, whereas that between 27 and

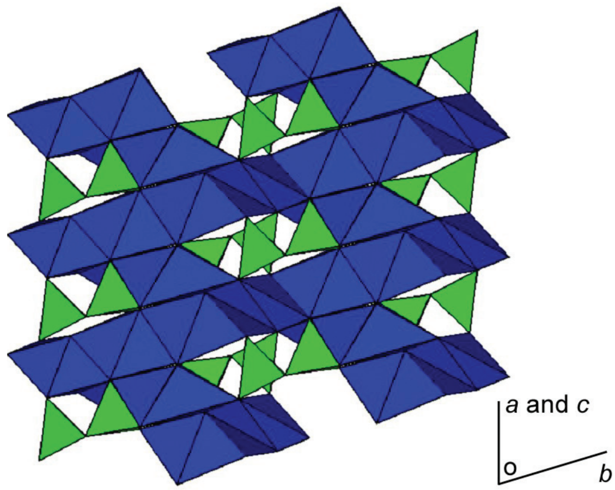

FIGURE 6. Structure of Wal, viewed down zone $[10\bar{1}]$. The Ca polyhedra are in blue, whereas the Si tetrahedra in green. The continuous CaO layers, running parallel to the *b*-axis, consist of eightfold Ca1 and sixfold Ca2 polyhedra (Joswig et al. 2003). These CaO layers are linked by the sevenfold Ca3 polyhedra and Si tetrahedra, the latter of which forms the characteristic Si_3O_9 rings in Wal. Atom labeling follows Joswig et al. (2003).

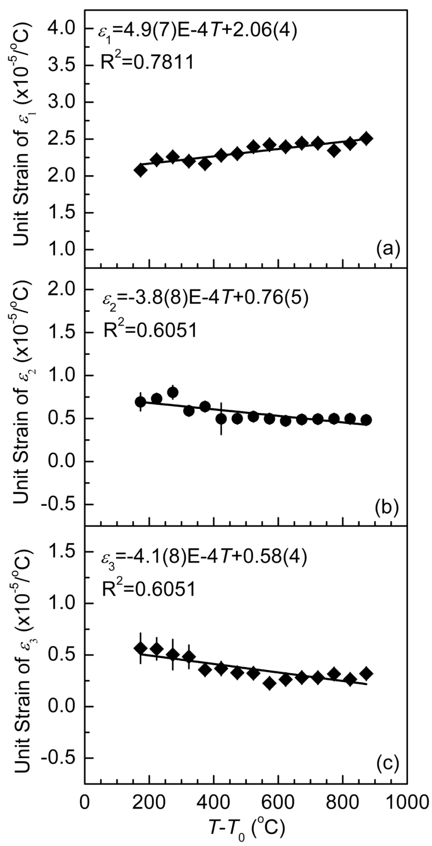

FIGURE 7. Magnitude of the three principal strains calculated at T-T_0, where *T* is the temperature of interest and T_0 is 27 °C. Note that lengths of the error bars are generally equal to or smaller than the symbols.

TABLE 3. Magnitude of the principal unit-strain coefficients (10^{-5}/°C), between room temperature and high *T*, and orientation (°) of the strain ellipsoid at high *T*

T-T_0	ε_1	ε_2	ε_3	ε_1:ε_2:ε_3	ε_1^a	ε_1^b	ε_1^c	ε_2^a	ε_2^b	ε_2^c	ε_3^a	ε_3^b	ε_3^c
173	2.08(9)	0.7(1)	0.6(1)	3.68:1.23:1	53(4)	37(3)	108(2)	96(27)	54(6)	45(31)	38(8)	96(19)	51(32)
223	2.22(6)	0.73(5)	0.6(1)	3.97:1.31:1	55(2)	35(2)	108(2)	69(18)	65(10)	19(8)	43(12)	112(10)	84(21)
273	2.26(8)	0.80(8)	0.5(1)	4.48:1.60:1	55(3)	34(2)	107(2)	64(13)	68(8)	18(3)	47(11)	115(8)	91(16)
323	2.20(7)	0.59(6)	0.5(1)	4.57:1.22:1	57(2)	37(2)	111(2)	61(30)	65(18)	22(3)	47(26)	115(18)	91(36)
373	2.17(4)	0.64(4)	0.36(6)	6.07:1.79:1	56(1)	36(1)	110(1)	59(6)	68(4)	20(2)	49(6)	117(3)	94(8)
423	2.28(6)	0.5(2)	0.37(7)	6.18:1.35:1	58(2)	37(3)	112(3)	52(23)	70(20)	25(14)	54(25)	119(13)	101(31)
473	2.30(3)	0.50(2)	0.33(5)	7.02:1.52:1	60(1)	37(1)	114(1)	57(9)	64(5)	24(2)	47(8)	115(5)	94(10)
523	2.40(4)	0.52(3)	0.32(6)	7.42:1.62:1	60(1)	37(1)	113(1)	47(8)	71(6)	29(7)	58(9)	120(5)	107(10)
573	2.42(3)	0.50(3)	0.23(5)	10.75:2.20:1	60(1)	37(1)	114(1)	55(5)	65(4)	25(2)	49(5)	116(3)	97(6)
623	2.40(3)	0.47(3)	0.26(5)	9.11:1.79:1	61(1)	38(1)	115(1)	53(7)	66(5)	27(3)	51(7)	117(4)	99(8)
673	2.45(2)	0.49(2)	0.28(3)	8.68:1.74:1	62(1)	39(1)	116(1)	50(5)	66(3)	29(3)	53(5)	118(3)	101(5)
723	2.45(2)	0.49(2)	0.28(4)	8.73:1.76:1	62(1)	39(1)	116(1)	53(5)	64(3)	27(2)	50(5)	116(3)	98(6)
773	2.35(2)	0.50(2)	0.32(3)	7.42:1.57:1	62(1)	39(1)	116(1)	37(4)	75(4)	39(4)	68(5)	125(2)	117(5)
823	2.44(3)	0.50(3)	0.26(4)	9.24:1.88:1	61(1)	39(1)	116(1)	51(6)	66(4)	28(3)	52(6)	118(4)	100(7)
873	2.51(2)	0.48(2)	0.32(4)	7.84:1.51:1	61(1)	40(1)	117(1)	43(5)	71(4)	33(4)	61(6)	124(3)	109(6)

900 °C is ε_1:ε_2:ε_3 = 7.8:1.5:1.

Natural Wal, discovered as inclusions in diamonds that probably originated from the lower mantle (Joswig et al. 1999; Jambor et al. 2000; Stachel et al. 2000; Nasdala et al. 2003; Brenker et al. 2005), has extreme degrees of LREE (200–2000 times chondritic) and Sr enrichment (70–1000 times chondritic) together with negative and positive Eu anomalies (Stachel et al. 2000), so that it could be a very important repository for these trace elements at high *P*. The enrichment of some trace elements in Wal is obviously related to the three large Ca sites in the Wal structure, which have different mean bond lengths of 2.521 (Ca3), 2.482 (Ca1), and 2.331 (Ca2) Å, respectively (Joswig et al. 2003). Another difference among these three Ca sites is their coordination number: 7 for Ca3, 8 for Ca1, and 6 for Ca2 (Joswig et al. 2003; Dörsam et al. 2009). High-*P* experiments have demonstrated that Sr substitutes Ca on all these three sites, with Ca3 as the most readily replaced, whereas Ca2 the most difficult one (Dörsam et al. 2009). Apparently, the size of the substituting cation, and the size and coordination number of the Ca site in the Wal structure all play a role in the substitution mechanism. Since Wal has a strong elastic anisotropy as demonstrated by this investigation, *T* and *P* might have strong effects on the substitution mechanism as well (Blundy and Wood 1994).

ACKNOWLEDGMENTS

We benefited from the discussions from two anonymous reviewers and Lars Ehm. This investigation was financially supported by the Fundamental Research Funds for the Central Universities from the Minister of Education of P. R. China (to X. Liu) and the National Natural Science Foundation of China (grant no. 41090371).

REFERENCES CITED

Akaogi, M., Yano, Y., Tejima, M., Iijima, M., and Kojitani, H. (2004) High-pressure transitions of diopside and wollastonite: phase equilibria and thermochemistry of $CaMgSi_2O_6$, $CaSiO_3$ and $CaSi_2O_5$-$CaTiSiO_5$. Earth and Planetary Science Letters, 143–144, 145–156.

Barkley, M.C., Downs, R.T., and Yang, H. (2011) Structure of walstromite, $BaCa_2Si_3O_9$, and its relationship to $CaSiO_3$-walstromite and wollastonite-II. American Mineralogist, 96, 797–801.

Blundy, J.D. and Wood, B.J. (1994) Prediction of crystal-melt partition coefficients from elastic moduli. Nature, 372, 452–454.

Brenker, F.E., Vincze, L., Vekemans, B., Nasdala, L., Stachel, T., Vollmer, C., Kersten, M., Somogyi, A., Adams, F., Joswig, W., and Harris, J.W. (2005) Detection of a Ca-rich litholgy in the Earth's deep (>300 km) convecting mantle. Earth and Planetary Science Letters, 236, 579–587.

Chatterjee, N.D., Johannes, W., and Leistner, H. (1984) The system CaO-Al_2O_3-SiO_2-H_2O: new phase equilibria data, some calculated phase relations, and their petrological applications. Contributions to Mineralogy and Petrology, 88, 1–13.

Dörsam, G., Liebscher, A., Wunder, B., Franz, G., and Gottschalk, M. (2009) Crystal structure refinement of synthetic $Ca_{0.43}Sr_{0.57}[SiO_3]$-walstromite and walstromite-fluid Ca-Sr distribution at upper-mantle conditions. European Journal of Mineralogy, 21, 705–714.

Essene, E. (1974) High-pressure transformations in $CaSiO_3$. Contributions to Mineralogy and Petrology, 45, 247–250.

Gasparik, T., Wolf, K., and Smith, C.M. (1994) Experimental determination of phase relations in the $CaSiO_3$ system from 8 to 15 GPa. American Mineralogist, 79, 1219–1222.

Henmi, C., Kusachi, I., Kawahara, A., and Henmi, K. (1978) 7*T* wollastonite from Fuka, Okayama Prefecture. Mineralogical Journal, 9, 169–181.

Henmi, C., Kawahara, A., Kenmi, K., Kusachi, I., and Takeuchi, Y. (1983) The 3*T*, 4*T* and 5*T* polytypes of wollastonite from Kushiro, Hiroshima Prefecture, Japan. American Mineralogist, 68, 156–163.

Hesse, K.-F. (1984) Refinement of the crystal structure of wollastonite-2*M* (parawollastonite). Zeitschrift für Kristallographie, 168, 93–98.

Hirose, K., Fei, Y., Ma, Y., and Mao, H. (1999) The fate of subducted basaltic crust in the Earth's lower mantle. Nature, 397, 53–56.

Huang, W.-L. and Wyllie, P.J. (1975) Melting and subsolidus phase relationships for $CaSiO_3$ to 35 kilobars. American Mineralogist, 60, 213–217.

Hu, X., Liu, X., He, Q., Wang, H., Qin, S., Ren, L., Wu, C., and Chang, L. (2011) Thermal expansion of andalusite and sillimanite at ambient pressure: a powder X-ray diffraction study up to 1000 °C. Mineralogical Magazine, 75, 363–374.

Ingrin, J. (1993) TEM imaging of polytypism in pseudowollastonite. Physics and Chemistry of Minerals, 20, 56–62.

Irifune, T., Susaki, J., Yagi, T., and Sawamoto, H. (1989) Phase transformations in diopside $CaMgSi_2O_6$ at pressures up to 25 GPa. Geophysical Research Letters, 16, 187–190.

Jambor, J.L., Kovalenker, V.A., and Roberts, A.C. (2000) New Mineral Names. American Mineralogist, 85, 873–877.

Joswig, W., Stachel, T.H., Harris, J.W., Baur, W.H., and Brey, G. (1999) New Ca-silicate inclusions in diamonds-tracer from the lower mantle. Earth and Planetary Science Letters, 173, 1–6.

Joswig, W., Paulus, E.F., Winkler, B., and Milman, V. (2003) The crystal structure of $CaSiO_3$-walstromite, a special isomorph of wollastonite-II. Zeitschrift für Kristallographie, 218, 811–818.

Kanzaki, M., Stebbins, J.F., and Xue, X. (1991) Characterization of quenched high pressure phases in $CaSiO_3$ system by XRD and ^{29}Si NMR. Geophysical Research Letters, 18, 463–466.

Kubo, A., Suzuki, T., and Akaogi, M. (1997) High pressure phase equilibria in the system $CaTiO_3$-$CaSiO_3$: stability of perovskite solid solutions. Physics and Chemistry of Minerals, 24, 488–494.

Kushiro, I. (1964) Wollastonite-pseudowollastonite inversion. Annual Report of the Director of the Geophysical Laboratory, Carnegie Institution of Washington, 1963–1964, 83–84.

Law, K.M., Blundy, J.D., Wood, B.J., and Ragnarsdottir, K.V. (2000) Trace element partitioning between wollastonite and silicate-carbonate melt. Mineralogical Magazine, 64, 651–661.

Liu, X., He, Q., Wang, H., Fleet, M.E., and Hu, X. (2010) Thermal expansion of kyanite at ambient pressure: an X-ray powder diffraction study up to 1000°C. Geoscience Frontiers, 1, 91–97.

Liu, X., Liu, W., He, Q., Deng, L., Wang, H., He, D., and Li, B. (2011) Isotropic thermal expansivity and anisotropic compressibility of ReB_2. Chinese Physics Letters, 28, 036401.

Mao, H.K., Yagi, T., and Bell, P.M. (1977) Mineralogy of the Earth's deep mantle: quenching experiments on mineral compositions at high pressure and temperature. Carnegie Institution of Washington Year Book, 76, 502–504.

Mazzucato, E. and Gualtieri, A.F. (2000) Wollastonite polytypes in the CaO-SiO_2 system. Part I. Crystallisation kinetics. Physics and Chemistry of Minerals, 27, 565–574.

Mikirticheva, G.A., Shitova, V.I., Petrov, S.A., Grabovenko, L.Y., Kuchaeva, S.K., and Grebenshchikov, P.G. (2001) Phase equilibria in the system $CaSiO_3$-$BaGeO_3$. Russian Journal of Applied Chemistry, 74, 1270–1273.

Nasdala, L., Brenker, F.E., Glinnemann, J., Hofmeister, W., Gasparik, T., Harris, J.W., Stachel, T., and Reese, I. (2003) Spectroscopic 2D-tomography: residual pressure and strain around mineral inclusions in diamonds. European Journal of Mineralogy, 15, 931–935.

Ohashi, Y. (1982) STRAIN: a program to calculate the strain tensor from two sets of unit-cell parameters. In R.M. Hazen and L.W. Finger, Eds., Comparative Crystal Chemistry, p. 92–102. Wiley, New York.

——— (1984) Polysynthetically-twinned structures of enstatite and wollastonite. Physics and Chemistry of Minerals, 10, 217–229.

Richet, P., Mysen, B.O., and Ingrin, J. (1998) High-temperature X-ray diffraction and Raman spectroscopy. Physics and Chemistry of Minerals, 25, 401–414.

Ringwood, A.E. (1975) Composition and Petrology of the Earth's Mantle. McGraw-Hill, New York.

——— (1994) Role of the transition zone and 660 km discontinuity in mantle dynamics. Physics of the Earth and Planetary Interiors, 86, 5–24.

Ringwood, A.E. and Major, A. (1967) Some high-pressure transformations of geophysical significance. Earth and Planetary Science Letters, 2, 106–110.

Stachel, T., Harris, J.W., Brey, G.P., and Joswig, W. (2000) Kankan diamonds (Guinea) II: lower mantle inclusion parageneses. Contributions to Mineralogy and Petrology, 140, 16–27.

Sueda, Y., Irifune, T., Yamada, A., Inoue, T., Liu, X., and Funakoshi, K. (2006) The phase boundary between $CaSiO_3$ perovskite and Ca_2SiO_4 + $CaSi_2O_5$ determined by in situ X-ray observations. Geophysical Research Letters, 33, L10307.

Swamy, V. and Dubrovinsky, L.S. (1997a) Thermodynamic data for the phases in the $CaSiO_3$ system. Geochimica et Cosmochimica Acta, 61, 1181–1191.

Swamy, V., Dubrovinsky, L.S., and Tutti, F. (1997b) High-temperature Raman spectra and thermal expansion of wollastonite. Journal of the American Ceramic Society, 80, 2237–2247.

Tamai, H. and Yagi, T. (1989) High-pressure and high-temperature phase relations in $CaSiO_3$ and $CaMgSi_2O_6$ and elasticity of perovskite-type $CaSiO_3$. Physics of the Earth and Planetary Interiors, 54, 370–377.

Trojer, T.J. (1968) The crystal structure of parawollastonite. Zeitschrift für Kristallographie, 127, 291–308.

Trojer, T.J. (1969) The crystal structure of a high-pressure polymorph of $CaSiO_3$. Zeitschrift für Kristallographie, 130, 185–206.

Wang, Y. and Weidner, D.J. (1994) Thermoelasticity of $CaSiO_3$ perovskite and implications for the lower mantle. Geophysical Research Letters, 21, 895–898.

Wenk, H.-R. (1969) Polymorphism of wollastonite. Contributions to Mineralogy and Petrology, 22, 238–247.

Yamanaka, T. and Mori, H. (1981) The structure and polytypes of α-$CaSiO_3$ (pseudowollastonite). Acta Crystallographica, B37, 1010–1017.

Yang, H. and Prewitt, C.T. (1999a) On the crystal structure of pseudowollastonite ($CaSiO_3$). American Mineralogist, 84, 929–932.

——— (1999b) Crystal structure and compressibility of a two-layer polytype of pseudowollastonite ($CaSiO_3$). American Mineralogist, 84, 1902–1905.

Manuscript received June 20, 2011
Manuscript accepted October 11, 2011
Manuscript handled by Lars Ehm